

Pulsed laser deposition of crystalline garnet waveguides at a growth rate of 20  $\mu\text{m}$  per hour

James A. Grant-Jacob\*, Stephen J. Beecher, Jake J. Prentice, David P. Shepherd, Jacob I.

Mackenzie and Robert W. Eason

Optoelectronics Research Centre, University of Southampton, Highfield, Southampton SO17

1BJ, UK

\*Corresponding author email: [jagj1v11@soton.ac.uk](mailto:jagj1v11@soton.ac.uk), Tel: 044 02380593186

Keywords: Pulsed laser deposition; Optical fabrication; Integrated optics; Laser materials;

Planar waveguides; Thin films

Abstract: We report pulsed laser deposition of high-quality crystalline yttrium aluminium oxide and yttrium gallium oxide with a growth rate approaching 20  $\mu\text{m}$  per hour by using an excimer laser operating at a repetition rate of 100 Hz. This result demonstrates the capability of PLD at 100 Hz for upscaling deposition speeds to a rate that is industrially relevant. In addition, we show that use of this high repetition rate can cause additional heating of the substrate, which in turn affects the film composition. This effect is used as an additional control parameter on the composition, and thus refractive index, of the grown material.

## 1. Introduction

Pulsed laser deposition (PLD) is a technique that uses laser pulses to ablate a target to form a plume of material which is then transferred to a substrate positioned nearby. PLD offers a variety of control parameters that can affect the thickness, quality and composition of the deposited material. As an example, the target composition, laser fluence and substrate temperature have been shown to affect the phase, stoichiometry and degree of crystallinity in a grown film. PLD has been used to deposit and grow a variety of materials, such as metal oxides [1], ferromagnetic materials [2], glasses [3] and, as discussed further in this work, crystalline optical materials [4,5].

Crystalline optical materials grown via PLD, have been shown to have very low propagation losses down to values of  $\sim 0.1$  dB/cm [6], though one limitation on growing optical films with desired properties is the ability to obtain the correct stoichiometry. However, as demonstrated previously, by pre-compensating a target to counteract specific elemental losses during transfer or evaporation during growth on the substrate, stoichiometric deposition can be achieved [7].

Optical films made of garnet materials such as yttrium aluminium oxide ( $\text{Y}_3\text{Al}_5\text{O}_{12}$ /YAG) are useful as solid-state laser hosts owing to their properties of high thermal conductivity and being optically isotropic [8]. In particular, erbium-doped yttrium gallium oxide ( $\text{Y}_3\text{Ga}_5\text{O}_{12}$ /YGG) is of interest owing to its spectroscopic properties, which are desirable in applications for both  $\text{CO}_2$  and methane gas detection in LIDAR (Light Detection And Ranging) systems [9–11]. One hurdle for PLD being used as an industrial and commercially viable process for films of thickness  $> 10$   $\mu\text{m}$ , is the rate of deposition. In this work, we present the hetero-epitaxial growth of single-crystal garnets on  $\langle 100 \rangle$ -oriented YAG substrates via pulsed laser deposition using laser repetition rates from 20 Hz up to 100 Hz.

In this paper, we show that high-quality single-crystal garnets can be grown by PLD at a deposition rate of 20  $\mu\text{m}$  per hour, and that, the increase in number of pulses when operating at

100 Hz contributes to heating of the substrate, which in turn affects the composition of the material in the grown film.

## **2. Experimental Setup**

Using a PLD setup discussed in previous work [12], laser pulses of  $\sim 20$  ns duration from a Coherent COMPexPro 110 excimer, operating at 20 – 100 Hz, were focused into a stainless-steel vacuum chamber, which was back filled with oxygen, onto a target material at a pulse energy of 100 mJ. The focused laser pulses resulted in a fluence of  $1.1 \text{ J cm}^{-2}$  on the target, which was rotated by an offset cam using a DC motor, in order to increase utilization of the surface area. The targets were 5-mm thick, 50-mm diameter, hot-pressed ceramic discs consisting of YAG, Er(1%):YGG or YGG. We also added an additional 2.5%  $\text{Al}_2\text{O}_3$  to the YAG target, 9.4%  $\text{Ga}_2\text{O}_3$  to the Er(1%):YGG target, and 12.7%  $\text{Ga}_2\text{O}_3$  to the YGG targets, in order to compensate for loss of Al and Ga respectively that routinely occurs during deposition.

The ablation plume produced was incident on surface-polished  $\langle 100 \rangle$ -orientated YAG substrates, of dimensions 10 mm $\times$ 10 mm $\times$ 1 mm, placed 6 cm away from the target. To enable crystalline growth of the deposited material, the substrates were heated using the output from a  $\text{CO}_2$  laser (10.6  $\mu\text{m}$  wavelength (IR), with a maximum output of 38 W), which was incident on the rear surface of the substrate [13]. The  $\text{CO}_2$  laser beam had a ‘top-hat’ spatial intensity profile, produced using a ZnSe tetraprism. This method has been routinely used to minimize both undesirable heat sinking and the total power required to heat the substrates, thereby avoiding undesirable vacuum chamber heating [14]. The substrates used here were heated by a  $\text{CO}_2$  laser power of 17.5 W, corresponding to a substrate temperature of  $\sim 600^\circ\text{C}$ , before deposition. All the garnet films, grown under the same conditions, though at different repetition rates of 20 Hz and 100 Hz for YAG and Er(1%):YGG, and 20, 40, 60, 80 and 100 Hz for YGG, were compared. The number of pulses for each deposition was kept constant at 36000, which corresponded to  $\sim 2 \mu\text{m}$ -thick films, sufficient for reliable X-ray diffraction (XRD) analysis, which was carried out using a Rigaku Smartlab X-ray diffractometer and Bruker D2 Phaser.

### 3. Results

#### 3.1. Depositions at 20 Hz and 100 Hz

##### 3.1.1. Crystallinity

X-ray diffraction spectra of the YAG and Er(1%):YGG films grown at 20 Hz and 100 Hz are shown in Fig. 1. The signal corresponding to the (400) peak from the YAG substrate at  $\sim 29.76^\circ$ , allows us to correctly determine the location of the (400) YGG and (400) YAG  $2\theta$  peaks from the grown samples, by making sure the (400) YAG  $2\theta$  peak from the substrate lines up to its database value of  $29.76^\circ$  [15]. Since the erbium dopant concentration is only 1% of the yttrium atoms in Er(1%):YGG, we use the (400) YGG peak as a point of reference for simplicity. The FWHM values of the peaks are similar when grown at 20 Hz compared with 100 Hz for both YAG ( $0.080^\circ$  and  $0.065^\circ$ , respectively) and Er(1%):YGG ( $0.036^\circ$  and  $0.031^\circ$ , respectively) films. For both materials, the 100-Hz XRD peak has a smaller  $2\theta$  value than the 20-Hz peak. This is attributed to the reduced Al and Ga content of the respective films, as already noted in [16], which occurs as a result of evaporation from the hot substrate. However, we do not think that the trend observed here for a reduced FWHM value for films grown at 100Hz is systematic, and at this stage do not have any reason to suspect improved crystal quality for such a higher repetition rate growth.

##### 3.1.2 Surface analysis

Measurements using a Zescope optical profiler to determine the number of particles of height  $> 20$  nm over a  $100\text{-}\mu\text{m} \times 100\text{-}\mu\text{m}$  area were taken along with roughness measurements to analyze surface quality, while the surface profiler enables the thickness of the materials to be determined. As an example of the surface morphology measurements taken of the films, Fig. 2 displays a 1-dimensional slice of the 2-dimensional optical profile data taken of the surface of YAG films grown at 20 Hz and 100 Hz, showing the greater surface roughness of the film grown at 20 Hz compared with 100 Hz. Table 1 displays a comparison of the particulate count, roughness and thickness of YAG and Er(1%):YGG films grown at 20 Hz and 100 Hz. As seen

from the table, for both targets, the number of particulates is fewer and the roughness is lower for films grown at 100 Hz, compared with the films grown at 20 Hz. The thickness of the samples is  $\sim 2 \mu\text{m}$  for all samples, indicating that (for the same total number of pulses) thickness is repetition rate independent. It can also be seen that growth rates of  $\sim 20 \mu\text{m}$  per hour are achievable at 100 Hz.

### *3.2 Repetition rate analysis*

To confirm the trend in higher deposition rate leading to a systematic decrease in  $2\theta$ , depositions were carried out at 20, 40, 60, 80 and 100 Hz. In this instance, we used an undoped YGG target, but with all other experimental conditions kept the same. XRD measurements were taken of 5 grown films, and the (400) YGG  $2\theta$  peak position value is displayed in Fig. 3 as a function of repetition rate. The black dashed-line at  $2\theta = 29.06^\circ$  corresponds to the  $2\theta$  database value of (400) YGG [15]. As seen from the plot, as the repetition rate increases, the XRD  $2\theta$  peak position decreases, with a total difference of  $\sim 0.04^\circ$  in  $2\theta$  from the 20 Hz to 100 Hz peak. From previous work [16], the shift in  $2\theta$  peak position has been observed to occur due to an increase in the  $\text{CO}_2$  laser-heated substrate temperature, which can cause gallium to be lost in the grown film through evaporation. By direct comparison, this difference in  $2\theta$  of  $\sim 0.04^\circ$  can easily be equated to an equivalent substrate-heating  $\text{CO}_2$  laser power of  $\sim 2.75 \text{ W}$ .

This proposed increase in heating due to increased repetition rate can be corroborated by examining the additional power burden transferred to the substrate as a result of the increased number of incident plumes per second when depositing at 100 Hz compared with 20 Hz. Since the plume takes some hundreds of  $\mu\text{s}$  to travel from the target to the substrate [17], which is shorter than the 10-ms time separation between each pulse at the maximum repetition rate of 100 Hz, subsequent pulses do not affect the plume dynamics of the previous pulse and each pulse can be considered as carrying equal kinetic energy to that at 20 Hz. Since the excimer laser is running in constant energy mode, i.e. the energy in each pulse remains the same, the kinetic energy in each plume is the same. Thus the systematic change observed in the XRD

peak position value, and therefore lattice spacing, must be due to an increasing number of pulses per second affecting the stoichiometry of the crystal. An extra 80 pulses incident on the target (at a pulse energy of 100 mJ), and thus an extra 80 plumes incident on the substrate per second, equates to a maximum of 8 W potentially transferred to the substrate.

Under the simplistic assumption that each particle within the plume has the same kinetic energy and that, the energy within the plume is converted to heat on deposition, the relative heating power delivered by the plume to the substrate can be estimated. Considering the ratio of the mass deposited on the 1-cm x 1-cm substrate compared with the total mass carried in the full extent of the plume, allows us to determine the additional level of heating that is generated by plume incidence on the substrate alone.

By depositing YGG over an unheated 75-mm x 50-mm glass substrate, the plume profile incident at the substrate plane was determined. A surface profile measurement of the deposited film, determined by measuring the interference fringes at a wavelength of 530 nm, is displayed in Fig. 4. Calculating the volume in the area of the sample (black dashed-line in a 1-cm x 1-cm square) versus the equivalent outside the sample region, the fraction of plume volume incident on the substrate is  $\sim 0.23$ . Since an additional 80 pulses per second is equivalent to a maximum additional 8 W incident on the target, if we assume all the incident laser energy is transferred into the plume, the 0.23 ratio gives an estimated additional heating of  $\sim 1.8$  W at 100 Hz, compared with 20 Hz deposition. This estimate along with the estimation from the shift in the XRD spectra as a function of substrate-heating CO<sub>2</sub> laser power, does indicate that the substrate is being heated by at an estimated additional  $\sim 1.8$  W.

This ability to controllably change the temperature of the substrate, and thus the exact composition of the material, potentially allows control of the refractive index of the material via the repetition rate, which is an interesting new concept in our view, since a change in composition clearly leads to a corresponding change in the refractive index of the grown material. Although we examined a range of repetition rates from 20 to 100 Hz, it is possible for

the laser to run at any integer value between 1 Hz and 100 Hz, thus allowing an even broader range and smaller incremental values of refractive indices to be contemplated. The repetition rate alone could thus be used to develop bespoke waveguides with tailored refractive index profile fabricated in a single PLD growth run.

#### **4. Conclusion**

We have documented the growth of garnet thin films on <100>-orientated YAG substrates using PLD at an ablation repetition rate of 100 Hz, producing crystalline quality as good as, or even superior, to that obtained at 20 Hz. Analysis of the thin film under the appropriate deposition conditions, shows that it is possible to grow these films at a rate of 20  $\mu\text{m}$  per hour. Our results demonstrate the possibility of either growing tens of films per day, or even > 100- $\mu\text{m}$ -thick single-crystal films in a single growth run of  $\sim 5$  hours. In addition, the increase in heating as a result of increase in the number of plumes incident on the sample per second at 100 Hz can cause an increase in lattice size as a result of evaporation of volatile elements from the film. There is therefore a direct correlation between the laser repetition rate used in PLD and the resultant refractive index via plume-induced substrate heating, which is a novel approach for sophisticated in-situ control of the material properties of PLD-grown films.

#### **Acknowledgements**

The authors acknowledge the support of the EPSRC through grant numbers EP/L021390/1, EP/N018281/1 and EP/J008052/1, the RDM data for this paper can be found at DOI: 10.5258/SOTON/D0144



## References

- [1] T.-W. Chiu, K. Tonooka, N. Kikuchi, Fabrication of ZnO and CuCrO<sub>2</sub>:Mg thin films by pulsed laser deposition with in situ laser annealing and its application to oxide diodes, *Thin Solid Films*. 516 (2008) 5941–5947. doi:<http://dx.doi.org/10.1016/j.tsf.2007.10.067>.
- [2] M. Gacic, H. Adrian, G. Jakob, Pulsed laser deposition of ferromagnetic Zn<sub>0.95</sub>Co<sub>0.05</sub>O thin films, *Appl. Phys. Lett.* 93 (2008) 152509. doi:[10.1063/1.3005413](https://doi.org/10.1063/1.3005413).
- [3] L. D'Alessio, R. Teghil, M. Zaccagnino, I. Zaccardo, D. Ferro, V. Marotta, Pulsed laser ablation and deposition of bioactive glass as coating material for biomedical applications, *Appl. Surf. Sci.* 138 (1999) 527–532. doi:[http://dx.doi.org/10.1016/S0169-4332\(98\)00610-2](http://dx.doi.org/10.1016/S0169-4332(98)00610-2).
- [4] A. Zakery, Y. Ruan, A. V Rode, M. Samoc, B. Luther-Davies, Low-loss waveguides in ultrafast laser-deposited As<sub>2</sub>S<sub>3</sub> chalcogenide films', *J, Opt. Sci. Am. B*, Vol. 20pp (2003) 1844–1852.
- [5] A. Choudhary, S.J. Beecher, S. Dhingra, B. D'Urso, T.L. Parsonage, J.A. Grant-Jacob, P. Hua, J.I. Mackenzie, R.W. Eason, D.P. Shepherd, 456-mW graphene Q-switched Yb:yttria waveguide laser by evanescent-field interaction., *Opt. Lett.* 40 (2015) 1912–5. doi:[10.1364/OL.40.001912](https://doi.org/10.1364/OL.40.001912).
- [6] C. Grivas, T.C. May-Smith, D.P. Shepherd, R.W. Eason, Laser operation of a low loss (0.1 dB/cm) Nd:Gd<sub>3</sub>Ga<sub>5</sub>O<sub>12</sub> thick (40 μm) planar waveguide grown by pulsed laser deposition, *Opt. Commun.* 229 (2004) 355–361. doi:[10.1016/j.optcom.2003.11.039](https://doi.org/10.1016/j.optcom.2003.11.039).
- [7] J.A. Grant-Jacob, S.J. Beecher, T.L. Parsonage, P. Hua, J.I. Mackenzie, D.P. Shepherd, R.W. Eason, Engineering of thin crystal layers grown by pulsed laser deposition, in: J.I. Mackenzie, H. Jelínková, T. Taira, M. Abdou Ahmed (Eds.), *Proc. SPIE 9893, Laser Sources Appl. III*, SPIE, Brussels, Belgium, 2016: p. 98930E. doi:[10.1117/12.2229747](https://doi.org/10.1117/12.2229747).
- [8] F.D. Patel, E.C. Honea, J. Speth, S.A. Payne, R. Hutcheson, R. Equall, Laser demonstration of Yb<sub>3</sub>Al<sub>5</sub>O<sub>12</sub> (YbAG) and materials properties of highly doped Yb:YAG, *IEEE J. Quantum Electron.* 37 (2001) 135–144. doi:[10.1109/3.892735](https://doi.org/10.1109/3.892735).
- [9] S.J. Beecher, J.A. Grant-Jacob, P. Hua, D.P. Shepherd, R.W. Eason, J.I. Mackenzie, Er:YGG Planar Waveguide Amplifiers for LIDAR Applications, in: *Lasers Congr. 2016 (ASSL, LSC, LAC)*, OSA, Washington, D.C., 2016: p. JTh2A.9. doi:[10.1364/ASSL.2016.JTh2A.9](https://doi.org/10.1364/ASSL.2016.JTh2A.9).
- [10] J.I. Mackenzie, J.A. Grant-Jacob, S.J. Beecher, H. Riris, A.W. Yu, D.P. Shepherd, R.W. Eason, Er:YGG planar waveguides grown by pulsed laser deposition for LIDAR applications, in: W.A. Clarkson, R.K. Shori (Eds.), *Proc. SPIE*, SPIE, San Francisco, United States, 2017: p. 100820A. doi:[10.1117/12.2256972](https://doi.org/10.1117/12.2256972).
- [11] T. Sakimura, Y. Watanabe, T. Ando, S. Kameyama, K. Asaka, H. Tanaka, T. Yanagisawa, Y. Hirano, H. Inokuchi, 3.2 mJ, 1.5 μm laser power amplifier using an Er, Yb: glass planar waveguide for a coherent Doppler LIDAR, in: *Proc. 17<sup>th</sup> Coherent Laser Radar Conf. Barcelona, Spain, Barcelona, Spain, 2013*.
- [12] J.A. Grant-Jacob, S.J. Beecher, H. Riris, A.W. Yu, D.P. Shepherd, R.W. Eason, J.I. Mackenzie, Dynamic control of refractive index during pulsed laser deposited

waveguide growth, *Opt. Mater. Express.* 7 (2017) 4073–4081. doi:10.1364/OME.7.004073.

- [13] T.C. May-Smith, A.C. Muir, M.S.B. Darby, R.W. Eason, Design and performance of a ZnSe tetra-prism for homogeneous substrate heating using a CO<sub>2</sub> laser for pulsed laser deposition experiments, *Appl. Opt.* 47 (2008) 1767. doi:10.1364/AO.47.001767.
- [14] K.A. Sloyan, PhD Thesis: Multi-beam pulsed laser deposition for engineered crystal films, University of Southampton, 2012. <http://eprints.soton.ac.uk/340246/>.
- [15] Inorganic Crystal Structure Database (ICSD), (n.d.). <http://icsd.cds.rsc.org> (accessed May 20, 2017).
- [16] J.A. Grant-Jacob, S.J. Beecher, D.P. Shepherd, R.W. Eason, J.I. Mackenzie, Tailoring the refractive index of films during pulsed laser deposition growth, in: E-MRS 2017 Spring Meet., Strasbourg, France, 2017: p. Q PW.15.
- [17] K.A. Sloyan, T.C. May-Smith, R.W. Eason, J.G. Lunney, The effect of relative plasma plume delay on the properties of complex oxide films grown by multi-laser, multi-target combinatorial pulsed laser deposition, *Appl. Surf. Sci.* 255 (2009) 9066–9070. doi:<http://dx.doi.org/10.1016/j.apsusc.2009.06.106>.

Table I

Quality analysis of Er(1%):YGG films grown at 20 Hz and 100 Hz.

Material	Repetition rate [Hz]	Particles > 20 nm	S <sub>a</sub> roughness [nm]	Thickness [μm]	Deposition rate [μm /hour]
YAG	20	110	4.138	2	4
	100	83	0.5	2	20
Er(1%):YGG	20	28	1.537	2	4
	100	2	0.469	2	20

Fig. 1. XRD spectra of YAG film grown at 20 Hz (blue dashed-line) and 100 Hz (blue solid-line), and Er(1%):YGG film grown at 20 Hz (green dashed-line) and 100 Hz (green solid-line). The black dashed-line indicates the  $2\theta$  database value of the (400) YAG peak.

Fig. 2. A 1-dimensional slice of the 2-dimensional optical profile data of the surface of YAG films grown at 20 Hz (blue solid-line) and 100 Hz (orange solid-line).

Fig. 3. (400) YGG  $2\theta$  peak position value as a function of repetition rate. The black-dashed line indicates the (400) YGG  $2\theta$  database value.

Fig. 4. Contour plot of thickness of YGG deposited on the glass slide, determined from interference fringes at a wavelength of 530 nm. The black dashed-square indicates the area of the 1-cm x 1-cm square  $\langle 100 \rangle$ -orientated YAG substrate within the plume.



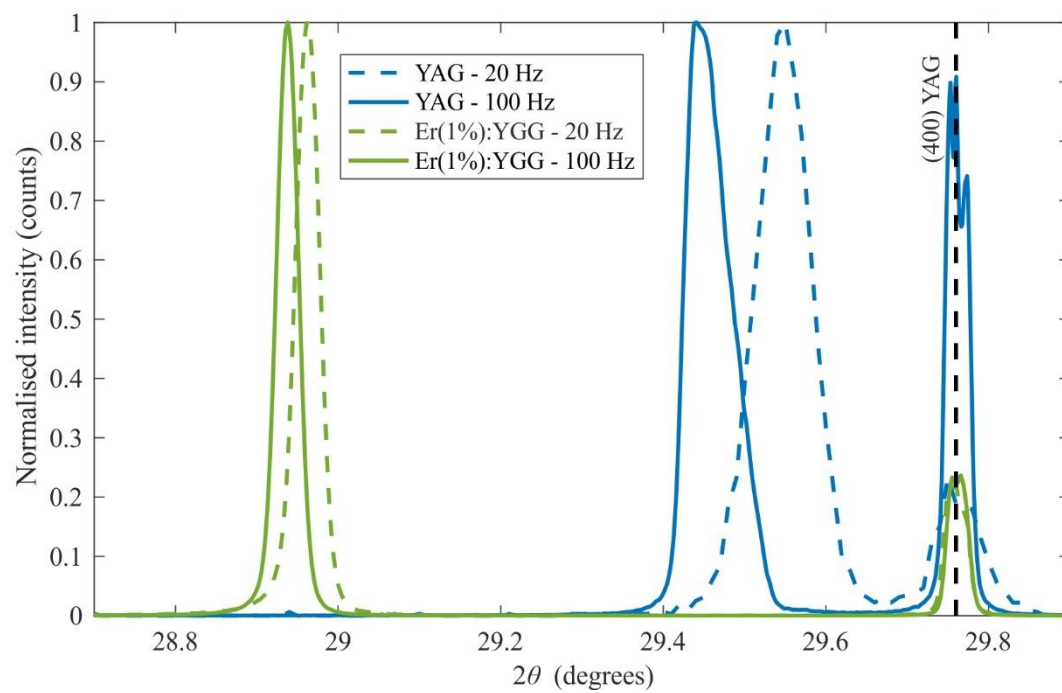


Fig. 1.

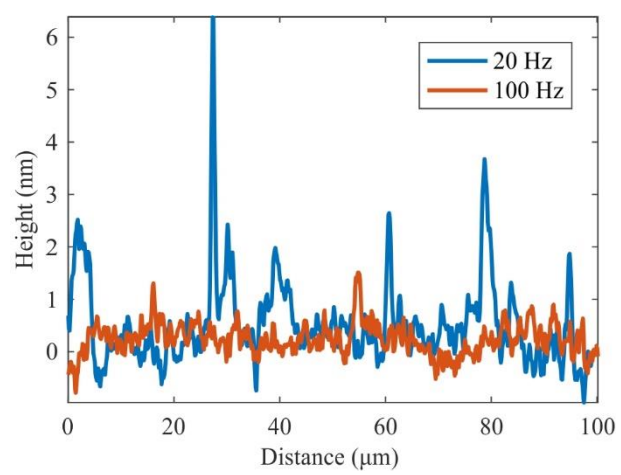


Fig. 2.

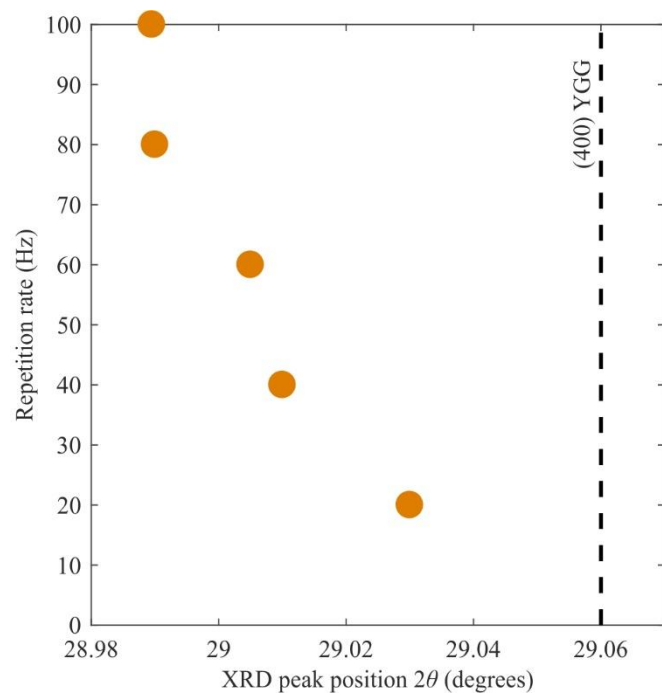


Fig. 3.



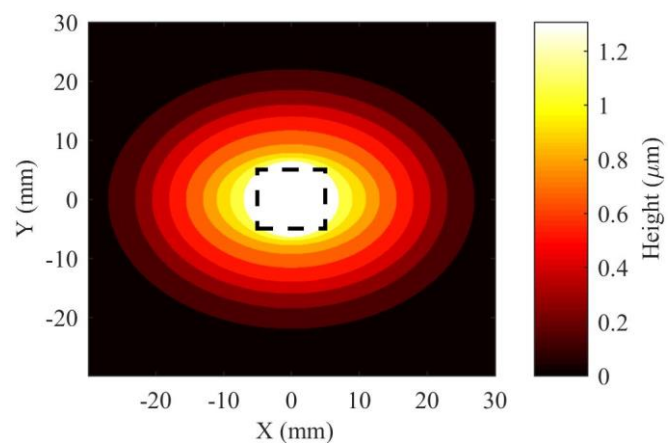


Fig. 4.